Computer Methods and Programs in Biomedicine 193 (2020) 105511

Contents lists available at ScienceDirect

Computer Methods and Programs in Biomedicine

journal homepage: www.elsevier.com/locate/cmpb

Clinical flexible needle puncture path planning based on particle swarm optimization

Chenxu Cai[a,b], Chunsheng Sun[a,b], Ying Han[a,b], Qinhe Zhang[a,b,*]

[a] Key Laboratory of High Efficiency and Clean Mechanical Manufacture (Ministry of Education), School of Mechanical Engineering, Shandong University, Jinan 250061, China

[b] National Demonstration Center for Experimental Mechanical Engineering Education, Shandong University, Jinan 250061, China

ARTICLE INFO

Article history:
Received 3 December 2019
Revised 24 March 2020
Accepted 14 April 2020

Keywords:
Flexible needle
Arc radius
Path planning
Particle swarm optimization

ABSTRACT

Background and objective: Percutaneous puncture with flexible needle has important value in clinical application for its low trauma and flexible path. However, it is difficult to guarantee accuracy and avoid obstacles in puncture process. Therefore, developing a viable path planning method is particularly important. In this research, the bending deformation law of flexible needles during puncture was studied and the puncture path was planned to provide a feasible method for clinical application of flexible needles.

Methods: According to the researchs that have been conducted, the path of the flexible needle in the tissue could be considered as a circular arc stitching. This research studied the calculation method of arc radius and obtained its actual value by the puncture experiments. Based on the arc model, the spatial transformation method of three-dimensional path planning was studied. In addition, a simplified particle swarm optimization (PSO) was applied into the process of path planning by changing the central angle of arc and the rotation angle of the needle body.

Results: The results of Experiment 1 showed that the path radius of the flexible needle pierced into gelatin prosthesis was influenced by four parameters, which were needle diameter, tip angle, puncture speed and the weight ratio of gelatin powder. As the needle diameter and tip angle increased, the radius of needle path tended to increase, but when the puncture speed and gelatin mass ratio increased, the radius of needle path decreased. The results of Experiment 2 showed that the distances of needle tip apart from target point were 3.2 mm (barrier-free experiments) and 1.8 mm (obstacle experiments).

Conclusions: This research links the intelligent algorithm with the flexible needle puncture tissue process, which has high value in future clinical application. By setting the correct boundary conditions and parameters, the flexible needle can be planned to reach the target point accurately.

1. Introduction

Percutaneous puncture is an important means of interventional therapy for cancer. The flexible needle is gradually applied to clinical surgery, for it is minimally invasive and its path can bypass important organs. It is important to study the deformation law of flexible needles in tissues and plan the puncture path to guarantee accuracy.

In the current studies about the deformation of the flexible needle, what can accurately explain the bending behavior of the flexible needle in the tissue is the cantilever model [1]. In addition, some studies analyzed the bending deformation of flexible needles from different aspects and established different mechanical models [2–5]. In view of the low rigidity of the flexible needle body, Webster III et al. [6] approximated the single-segment trajectory of the flexible needle in the tissue to circle arc. During the puncture process, the main factor that causes the needle to bend is the inclination of the needle tip. The orientation of needle bevel which can be changed by rotating the needle body determines the bending direction of the needle. Therefore, during the puncture process, the needle path can be controlled by rotating the needle body [7,8]. In the studies of the puncture path of the flexible needle, the main model is bicycle motion model, in which, the puncture trajectory of the flexible needle is regarded as a curve formed by the stitching of multiple arcs. The transformation between each arc is achieved by rotating the needle body

* Corresponding author at: School of Mechanical Engineering, Shandong University, No. 17923, Jingshi Road, Jinan 250061, China.
E-mail address: zhangqh@sdu.edu.cn (Q. Zhang).

https://doi.org/10.1016/j.cmpb.2020.105511
0169-2607/

[9]. Many studies made considerable progress based on this model [10–13]. In addition to the arc model, Park W et al. [14] adapted the path-of-probability (POP) algorithm to path planning of flexible needles with bevel tips. They controlled the trajectory of the flexible needle by rotating the needle body. Their research solved the path planning problem for flexible needles in more general cases that included obstacles. Pedro et al. [15] presented a flexible needle steering system that combined an MR-compatible robot with a Fiber Bragg Grating (FBG)-based needle tip tracker, and improved puncture accuracy by closed-loop method. Zhang et al. [16] glued the strain gauges on the needle surface to achieve real-time detection of needle bending. In recent years, intelligent algorithms are applied to flexible needle path planning, such as rapidly-exploring random tree algorithm [17–18] and Markov decision processes [19]. Compared with these algorithms, the particle swarm algorithm is simpler and more directional. In addition, parameters of PSO can be easily adjusted when the boundary conditions change. Because of its advantages, PSO has been widely used in industrial path planning [20–21]. When PSO algorithm is applied to flexible needle path planning, the path can be obtained by changing the most basic elements of the path, such as the length of each arc and the angle between adjacent arcs. In this way, the path is simpler and more efficient. In view of these advantages of particle swarm optimization, it is chosen to plan the flexible needle path in this paper. Previous studies have proven that it is feasible to apply the PSO algorithm to flexible needle path planning [22].

In this paper, as the single-segment trajectory of a flexible needle is approximated into circular arc, the spatial transformation method of three-dimensional path planning is studied. A simpler PSO than existing research is used by controlling the central angle of a single arc and rotation angle of the needle body between adjacent arcs. Puncture experiments are carried out to probe puncture accuracy of the algorithm under certain conditions.

2. Flexible needle trajectory model

2.1. Calculation of path radius

The path of flexible needle is regarded as a three-dimensional curve of multi-section arc splicing due to its low rigidity. The value of the single arc radius cannot be directly measured in the experiment but can be obtained by measuring the bending deflection of the needle tip under certain puncture situation. The relationship between various parameters is shown in Fig. 1.

The following equations can be obtained from Fig. 1:

$$\theta_R = \frac{L}{R} \tag{1}$$

$$\cos\theta_R = \frac{R-\omega}{R} \tag{2}$$

Where, R is the radius of the needle path, L is the length of the needle in tissue, ω is the tip deflection, and θ_R is the central angle from the piercing point to the needle tip. Radius calculation equation can be obtained by substituting Eq. (1) into Eq. (2):

$$\cos\frac{L}{R} = 1 - \frac{\omega}{R} \tag{3}$$

It is revealed from Eq. (3) that the radius of the needle path can be obtained by controlling the penetration depth and measuring the deflection of the needle tip in the experiment.

2.2. Three-dimensional path model

In order for the flexible needle to puncture a predetermined path in tissue, a certain method is needed for the three-dimensional path planning. In this paper, the basic idea is to decompose the 3D path planning problem into 2D. Single-segment arc is planned in one plane, and 3D path is obtained by changing the planning plane. The transformation of adjacent arc planes needs to be achieved by rotating needle, wherein the angle between the two planes is related to the rotation angle. The three-dimensional puncture path planning method is shown in Fig. 2.

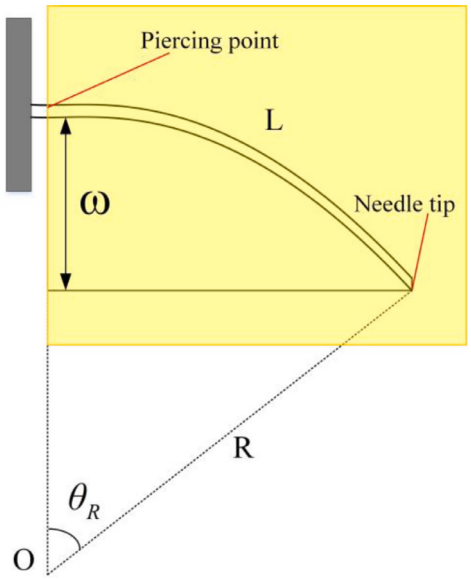

Fig. 1. Radius calculation geometry diagram.

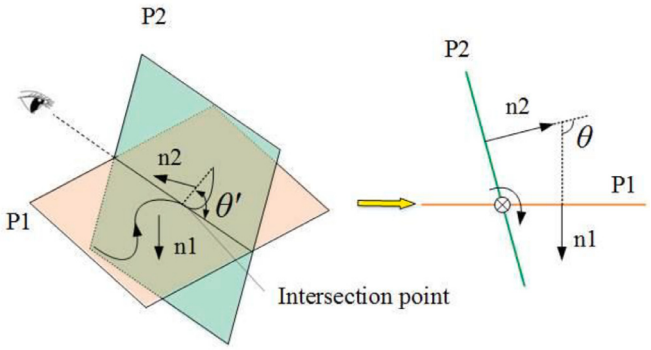

Fig. 2. 3D puncture path conversion diagram.

In Fig. 2, **n1** and **n2** are the normal vectors of planes P1 and P2, respectively. The angle between **n1** and **n2** is θ in degrees. Intersection point is the connection point between the paths in plane P1 and in plane P2. When the flexible needle is punctured in a plane, the direction of the plane normal vector satisfies the right-hand rule related to the trajectory of the needle.

At the beginning, the flexible needle is punctured in plane P1. When the flexible needle is punctured at the intersection point, it needs to be rotated counterclockwise $\theta_{ccw} = \theta$ or clockwise θ_{cw} = 360-θ in degrees. The planning plane is converted to P2.

If the unit direction vector of the arc tangent at the intersection point is **A**, the new vector **P'** can be obtained by rotating the space vector **P** around vector **A** for θ_{ccw} degrees. The equation is shown as follow:

$$P' = P\cos\theta_{ccw} + A \times P\sin\theta_{ccw} + A(A\cdot P)(1-\cos\theta_{ccw}) \tag{4}$$

According to Eq. (4), if the coordinates of the previous segment arc center and the intersection point are known, the coordinates of the new arc center can be obtained.

It should be noted that the coordinates of the points on the space arc cannot be acquired directly from MATLAB. The

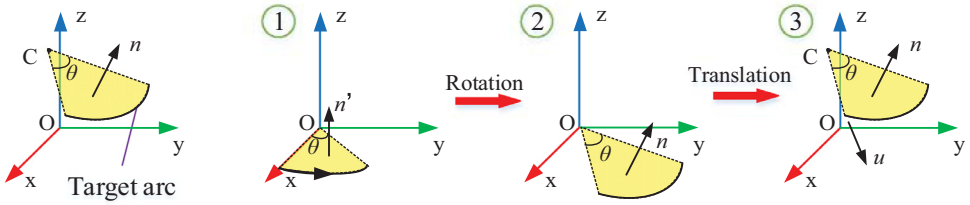

Fig. 3. Arc conversion process in MATLAB.

coordinates of the points on the circle on X-Y plane should be obtained by polar method preliminarily. Then, the translation matrix *Tt* and the rotation matrix *Tr* are used to calculate coordinates of target arc points. The process is shown in Fig. 3.

Assuming that the coordinates of the circle center is (*C*1, *C*2, *C*3), the unit vector from the arc center to initial point of the arc is $\vec{u} = (ux, uy, uz)$; the unit normal vector of the target plane is $\vec{n} = (nx, ny, nz)$; and it should be noted that $\vec{n} \times \vec{u} = (vx, vy, vz)$. *Tt* and *Tr* are given by the equations as follow:

$$Tt = \begin{bmatrix} 1 & 0 & 0 & C1 \\ 0 & 1 & 0 & C2 \\ 0 & 0 & 1 & C3 \\ 0 & 0 & 0 & 1 \end{bmatrix} \tag{5}$$

$$Tr = \begin{bmatrix} ux & uy & uz & 0 \\ nx & ny & nz & 0 \\ vx & vy & vz & 0 \\ 0 & 0 & 0 & 1 \end{bmatrix} \tag{6}$$

Assuming that (*x, y, z*) are the coordinates of the point on the arc, and (x0, y0, z0) are the coordinates of the arc point planned in X-Y plane. The coordinates of the points on any arc in space are obtained by the equation as follow:

$$(x, y, z, 1) = Tt \cdot Tr \cdot (x0, y0, z0, 1) \tag{7}$$

3. Path planning based on PSO

The basic idea of PSO is firstly obtaining a number of random particles (initial population) through the way of uniform distribution, secondly setting the objective function, and finally obtaining the optimal solution of the objective function.

As the PSO is used in three-dimensional path planning in this paper, two variables need to be defined as particles, which are the values of the center angle of each arc and the angle of rotation of the needle body between adjacent arcs. With the two variables and radius of the arc, the coordinates of any point on space arc are calculated.

The objective function contains two optimization targets. One is the distance between the target point and the end point of the path, the other is whether the path collides with obstacle points. The objective function is given as follow:

$$Fx = \begin{cases} \left| \vec{n}_{endnode} - \vec{n}_{targetnode} \right| & (COL = 0) \\ +\infty & (COL = 1) \end{cases} \tag{8}$$

In Eq. (8), $\vec{n}_{endnode}$ is the coordinate vector of the end point; $\vec{n}_{targetnode}$ is the coordinate vector of the target point. *COL* is the collision variable which reflects whether the needle path collides with an obstacle point. The initial value of *COL* is 0. The value of *COL* is changed to 1when the needle path collides with an obstacle point. The process of using the PSO to perform puncture path planning in MATLAB is shown as follows:

Step one: Initial data such as coordinates of the starting point and the target point, initial piercing direction, population size, the maximum number of iterations and the number of rotating needle *d* (spatial dimension) are set; the X-Y plane is defined as basic planning plane.

Step two: The range of the central angle and rotation angle of the needle body are defined. The value of such angles (particles) and the initial flight speed are randomly generated by uniform distribution law. The form of each particle is (θ_{Y1},θ_{Y2},...$\theta_{Y(d+1)}$; θ_{Z1},θ_{Z2},...θ_{Zd}), where θ_{Yi}(i=1, 2... d + 1) is the central angle of the corresponding arc, and θ_{Zi} (i=1, 2... d) is the angle of rotation of the needle body.

Step three: The objective function of each particle is calculated to get the best fitness of the current population. If the value of objective function is the smallest, then the corresponding particle is the current optimal particle. If the end point of this particle is less than 2 mm apart from the target point, then the iteration is stopped, and the process jumps to step six.

Step four: The current optimal particle is compared with the historical optimal solution. If the current optimal particle is better than the historical optimal particle, the historical optimal particle is updated to the current optimal particle.

Step five: The flying speed of the next iteration and the new particle position is calculated. If the number of iterations hasn't reached the maximum value, the process jumps to step three.

Step six: The data of the optimal particle is selected to conduct experiment.

4. Comparative simulation

Rapidly-exploring random tree (RRT) is one of the mainstream algorithms. It was chosen by many researchers as flexible needle path planning algorithm because of its high speed and accuracy [17,23]. In order to prove that PSO has advantages in flexible needle path planning, RRT is selected as the comparison algorithm.

In this paper, the performance of the two algorithms is compared through simulation. The coordinates of the initial point is set to (0, 0, 0); the coordinates of the target point is set to (0, 120, 0); the penetration angle is 0°; the radius of needle path is set to 50 mm. A spherical obstacle is set in the simulation. The coordinates of the obstacle's center is (0, 70, 0), and the diameter of the obstacle is 5 mm. In the path planning using PSO, the population size is 70. In the path planning using RRT, the step length is 50 mm. The simulation results are shown in Fig. 4 and Table 1.

It can be seen from simulation results that the path planning of flexible needles using RRT has higher accuracy than using PSO.

Table 1
Planning results of PSO and RRT

Algorithm	Error(mm)	Number of arc segments	Total path length(mm)
RRT	0	9	123.98
PSO	1.38	3	126.82

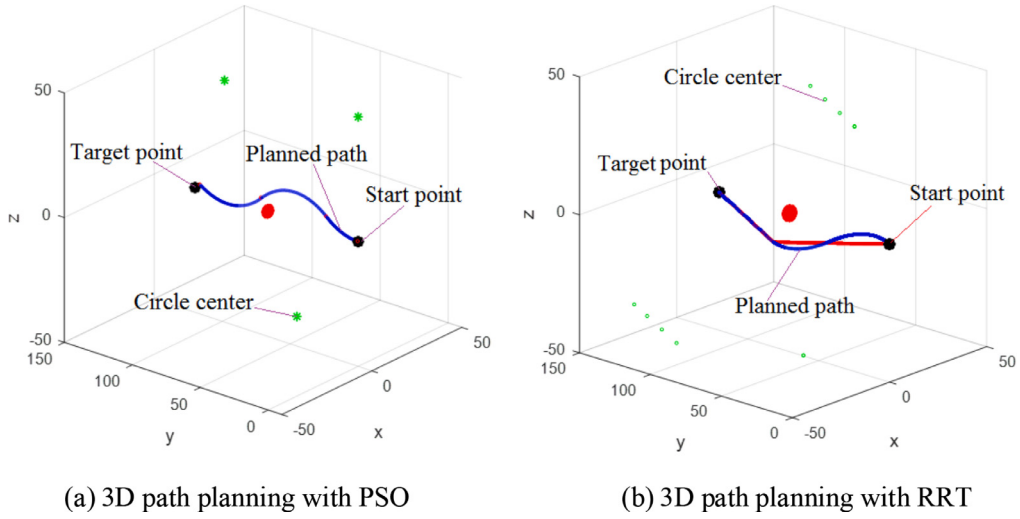

(a) 3D path planning with PSO (b) 3D path planning with RRT

Fig. 4. Path planning simulation in MATLAB.

In terms of the number of arc segments, RRT is significantly more than PSO. The total path lengths are not much different.

When PSO is used for path planning, the planning is completed when the distance between the end point of the path and the target point is less than the specified value, while the algorithm calculation method of RRT can make the path reach the target point accurately. Therefore, it is reasonable that RRT is slightly more accurate than PSO in simulation. As long as the puncture accuracy is within the allowable range, it can be considered feasible. The number of arc segments, in other words, the times of rotation of the needle body, is a parameter worth considering. It is because that the radius of the path is an approximate value calculated under large bending deformation of flexible needle. Rotating needle body frequently makes the actual radius of the path larger than the calculated value, resulting in a decrease in the final puncture accuracy. In addition, excessive needle rotations also cause great pain to patients during surgery. For RRT, it is difficult to determine the appropriate step length when the target point is changed, which caused RRT to be less versatile than PSO in flexible needle path planning.

To sum up, PSO has obvious advantages over RRT in flexible needle path planning.

5. Experimental device and methods

In this paper, the puncture experiments are mainly divided into two parts. The purpose of Experiment 1 is to find the radius of flexible needle path under different puncture parameters and select the appropriate puncture parameters for path planning. The purpose of Experiment 2 is to explore the puncture error of PSO path planning method under certain conditions.

5.1. Experimental device

The experimental device is shown in Fig. 5. In the control system, Mitsubishi PLC was used as the main controller, and the touch screen was used to input the puncture data. The three-degree-of-freedom puncture platform was used to comply the linear feed of the flexible needle, the rotation of the needle body, and the adjustment of the piercing angle. The two-degree-of-freedom ball screw workbench was used to adjust the position of the puncture material in the horizontal direction. For the convenience of observation, the puncture material used in the experiment was a gelatin prosthesis which was similar to human organs and tissues in mechanical properties.

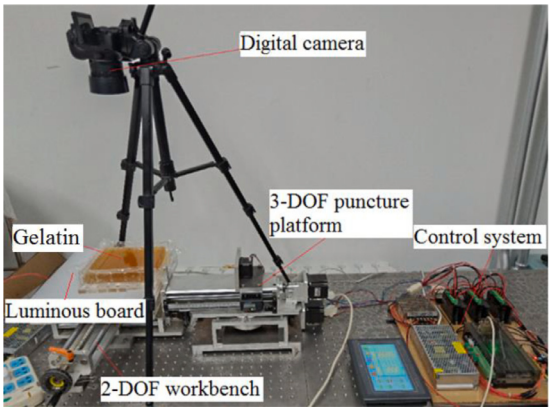

Fig. 5. Experimental device.

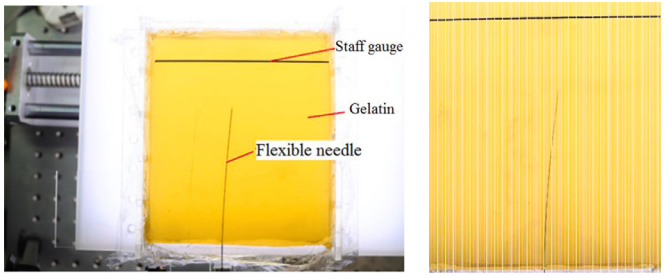

(a) Original photo (b) Processed image

Fig. 6. Radius measurement experiment figure.

5.2. Measuring method of radius

In the experiment, a staff gauge which was 140 mm long was placed on the surface of the gelatin for measuring the deflection of needle tip. The process was photographed when gelatin was pierced by flexible needle, and the photos were processed by MATLAB software so that the deflection of the needle could be read by counting the number of grids as shown in Fig. 6. At the same time, the actual needle length of the flexible needle was read from an electronic ruler. The radius of the needle path was calculated according to Eq. (3).

Table 2
Experiment 1.1 - change the diameter of the needle.

Experiment number	Mass ratio	Needle diameter (mm)	Tip angle (In degree)	Puncture speed (mm/s)
1	18%	0.7	20	4
2	18%	0.6	20	4
3	18%	0.55	20	4

Table 3
Experiment 1.2 - change the tip angle.

Experiment number	Mass ratio	Needle diameter (mm)	Tip angle (In degree)	Puncture speed (mm/s)
1	18%	0.6	60	4
2	18%	0.6	45	4
3	18%	0.6	20	4
4	18%	0.6	15	4

Table 4
Experiment 1.3 - change the puncture speed.

Experiment number	Mass ratio	Needle diameter (mm)	Tip angle (In degree)	Puncture speed (mm/s)
1	18%	0.6	20	1
2	18%	0.6	20	4
3	18%	0.6	20	7
4	18%	0.6	20	10
5	18%	0.6	20	13

Table 5
Experiment 1.4 - change the gelatin powder mass ratio.

Experiment number	Mass ratio	Needle diameter (mm)	Tip angle (In degree)	Puncture speed (mm/s)
1	6%	0.6	20	4
2	12%	0.6	20	4
3	18%	0.6	20	4

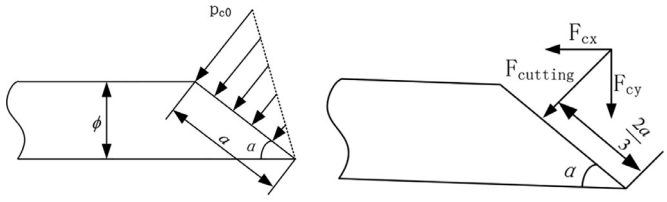

(a) Tip force distribution (b) Simplifying of tip force

Fig. 7. Force on needle tip during puncture.

5.3. The parameters of Experiment 1

The force applies to the needle tip as the flexible needle punctured gelatin is shown in Fig. 7. It can be seen from the picture that the diameter of the needle and the tilt angle of the needle tip influence the force situation on the needle tip. At the same time, puncture speed and mechanical properties of gelatin prosthesis affect the value of tip force.

Four parameters including the diameter of flexible needle, the needle tip tilt angle, the puncture speed and the mass ratio of gelatin powder have a great influence on the radius of the needle path. The radius of the needle path under different value of parameters was obtained to explore the influence of parameters on the path radius. The experimental parameters were set as shown in Tables 2–5. Each parameter were repeated three times in experiment.

5.4. Parameter of puncture experiment using PSO

According to the data obtained from Experiment 1, a 23G flexible needle with 0.6 mm diameter was selected for path planning experiments. The tip angle of the needle was 20°; the gelatin mass ratio was 18%; and the puncture speed was 4 mm/s. The radius was 553.7 mm with the selected parameters. For convenience of observation, the experiment mainly focused on two-dimensional path planning.

Experiment 2 was divided into two parts: barrier-free experiment and obstacle experiment. In the barrier-free experiment, the planning plane was set to the plane of $Z = 0$; the normal vector of the first arc was (0, 0, 1); the coordinates of the piercing point was (0, 0, 0); the coordinates of the target point was (-5, 120, 0); the number of arc segments was 2; and the piercing angle was 0°.

In the obstacle experiment, the coordinates of the obstacle whose radius was R=2 was set to (0, 70, 0). The coordinates of the piercing point was (0, 0, 0); the coordinates of the target point was (0,120, 0); the penetration angle was 5°; the number of arc segments was 3; the population size was 50; and the maximum number of iterations was 1000.

6. Experimental results and discussion

6.1. Relationship between experimental parameters and radius

In Experiment 1, the flexible needle diameter, the tip tilt angle, the puncture speed and the gelatin powder mass ratio were changed. The deflection of the flexible needle tip under different parameters was measured, and the radius under the corresponding parameters was calculated as shown in Fig. 8.

It can be seen from Fig. 8(a) that the increase of the diameter of the flexible needle makes the bending radius increase. When the needle diameter increases from 0.55 mm by 27% to 0.7 mm, the bending radius of the needle path increases from 524.65 mm to 739.27 mm, where the value increases by 41%. It can be explained that the increase of needle diameter will increase the cutting force

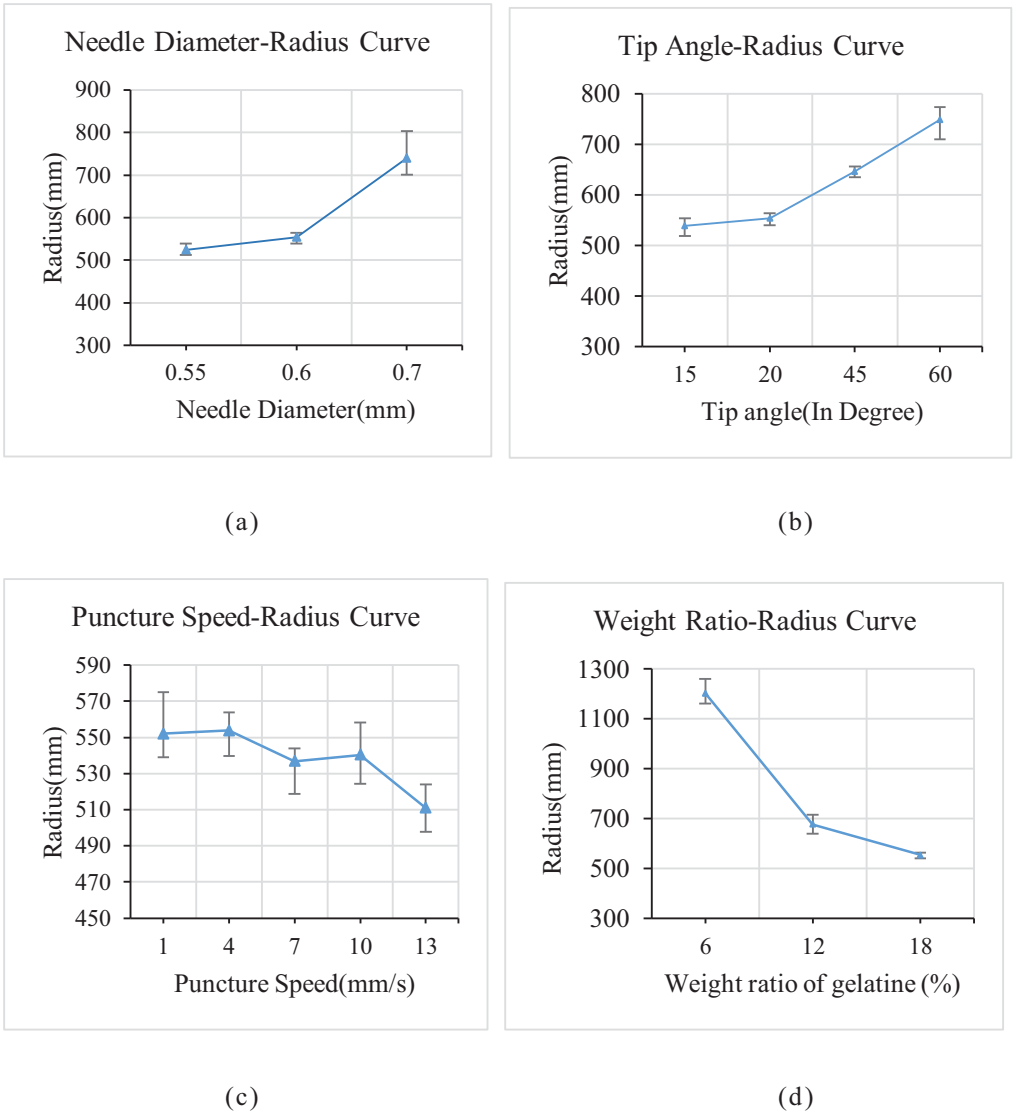

Fig. 8. The radius under different parameters.

of the needle tip linearly, but at the same time, the increase of the diameter will increase the moment of inertia in the fourth power. The effect of the increase in tissue cutting force is not sufficient to resist the influence of the increase in moment of inertia, so the radius tends to increase as the diameter of the needle increases.

It can be seen from Fig. 8(b) that as the inclination angle of the needle tip increases, the radius increases. In the range of 15° to 60°, the path radius of the needle gradually increases from 538.67 mm to 749.73 mm, and the curve is roughly proportional. It can be seen from Fig. 7 that the increase of the tip angle reduces the component of the puncture force in the radial direction.

As can be seen from Fig. 8(c), with the increase of the puncture speed, the radius of the needle path shows a declining trend. When the puncture speed is 4 mm/s and 1 mm/s, the path radii are almost the same. When the puncture speed increases to 10 mm/s, the radius increases compared with 7 mm/s. As a whole, when the speed increases from 1 mm/s to 13 mm/s, the path radius decreases from 551.97 mm to 510.95 mm, which decreases by 7%. This is because that the increase of the puncture speed will increase the puncture force. But compared with other variables, the impact of force on radius is lighter.

As can be seen from Fig. 8(d), when the gelatin mass ratio increases from 6% to 12%, the radius of the needle path decreases from 1202.5 mm to 676.7 mm, a drop of almost half. When the gelatin mass ratio increases to 18%, the needle path radius decreases to 553.8 mm, where the decrease value is reduced to 18%. The elasticity and toughness of the gelatin prosthesis increase when the gelatin mass ratio increases. If other conditions are constant, the force which the needle requires to cut the gelatin increases. According to Newton's second law, the force that gelatin applies to the needle tip is larger, so the bending degree of the needle is larger.

6.2. Result of puncture experiment using PSO

The result of barrier-free experiment is shown in Fig. 9. According to the simulation result, the length of the first arc was 50.9 mm and that of the second was 68.5 mm. As the planning plane was $Z = 0$, the actual coordinates of the target point was (-4.5, 120) in experiment; the coordinates of the needle tip was (-2.0, 119.0) as shown in Fig. 9(b). Needle tip was 3.2 mm apart from the ideal target point.

The result of obstacle experiment is shown in Fig. 10. According to the simulation result, the lengths of the three section arcs were 14.75 mm, 11.85 mm and 93.05 mm in turn. The data was input into the puncture platform for puncture experiment. In

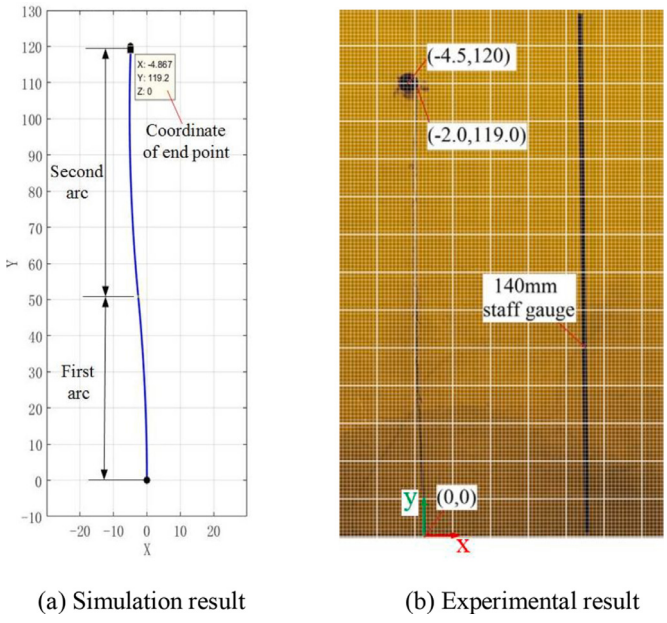

Fig. 9. Barrier-free path planning.

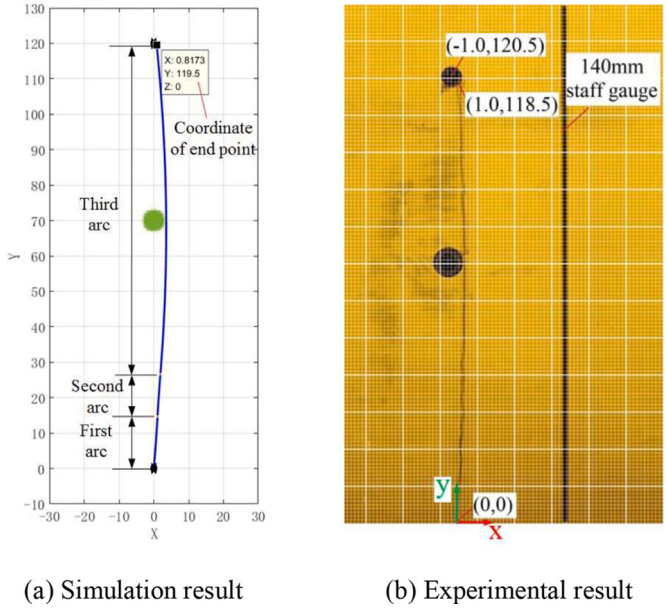

Fig. 10. Obstacle path planning.

experiment, the coordinates of the actual target point was (-1.0, 120.5), and the coordinates of the needle tip was (1.0, 118.5). The needle tip was 1.8 mm apart from the ideal target point.

In the experiments base on PSO, the coordinates of end points on the actual path are slightly different from simulation. It is because the actual trajectory of the flexible needle is not ideal arc. When the trajectory is simplified to an arc, it is inevitable that an error will occur. But it can be seen from experiments that the error is within acceptable range, and the final puncture error is controlled within 4 mm, which meets the accuracy requirement.

7. Conclusion

In this paper, the radius of the flexible needle path under four parameters was studied through puncture experiment, and the influence of each parameter on the radius was briefly discussed. The experimental results show that the increase of the diameter of the flexible needle and the inclination angle of the needle tip makes the radius increase; the increase of the puncture speed will slightly decrease the radius; when the mass ratio of gelatin increases, the radius is greatly reduced. At the same time, the application of particle swarm optimization algorithm in flexible needle puncture path was analyzed, and the method of planning in MATLAB was given. Finally, the puncture experiments under barrier-free and obstacle conditions were conducted. In the experiment, puncture errors are both within 4 mm, which meet the accuracy requirements.

Declaration of Competing Interest

The authors declare no conflict of interest.

Acknowledgments

This material was based upon the work supported by the National Natural Science Foundation of China (grant no. 51475274), the Natural Science Foundation of Shandong Province (ZR2019MEE017), the Key R&D Program of Shandong Province (2019GHZ002) and the National Key R&D Program of China (2019YFC0119200).

References

[1] D. Gao, Y. Lei, H. Zheng, Needle steering for robot-assisted insertion into soft tissue: a survey, Chin. J. Mech. Eng. 25 (4) (2012) 629–638, doi:10.3901/CJME.2012.04.629.
[2] B. Konh, P. Hutapea, Finite element studies of needle–tissue interactions for percutaneous procedures, J. Med. Devices 9 (3) (2015) 030941-030941-2, doi:10.1115/1.4030573.
[3] B. Konh, M. Honarvar, et al., Simulation and experimental studies in needle–tissue interactions, J. Clin. Monit. Comput. 31 (4) (2017) 861–872, doi:10.1007/s10877-016-9909-6.
[4] T. Lehmann, M. Tavakoli, N. Usmani, et al., Force-sensor-based estimation of needle tip deflection in brachytherapy, J. Sens. 2013 (2013) 529–544, doi:10.1155/2013/263153.
[5] W. Dong, H.M. Han, Z.J. Du, The tip interface mechanics modeling of a bevel-tip flexible needle insertion, in: IEEE International Conference on Mechatronics and Automation, Piscataway, USA, IEEE, 2012, pp. 581–586, doi:10.1109/ICMA.2012.6283172.
[6] R.J. Webster, J.S. Kim, N.J. Cowan, G.S. Chirikjian, A.M. Okamura, Nonholonomic modeling of needle steering, Int. J. Robot. Res. 25 (5-6) (2006) 509–525, doi:10.1177/0278364906065388.
[7] P.S. DiMaio, S.E. Salcudean, Needle steering and motion planning in soft tissues, IEEE Trans. Biomed. Eng. 52 (6) (2005) 965–974, doi:10.1109/TBME.2005.846734.
[8] Q. Yao, X. Zhang, Duty-cycled spinning based 3D motion control approach for bevel-tipped flexible needle insertion, J. Mech. Med. Biol. 18 (7) (2018) SI, doi:10.1142/S0219519418400171.
[9] R.J. Webster, J. Memisevic, A.M. Okamura, Design considerations for robotic needle steering, in: Proceedings of the 2005 IEEE, International Conference on Robotics and Automation, Barcelona, Spain, 2005, pp. 3599–3605.
[10] J. Carriere, M. Khadem, C. Rossa, et al., Event-triggered 3D needle control using a reduced-order computationally efficient bicycle model in a constrained optimization framework, J. Med. Robot. Res. 4 (1) (2018) 1–16, doi:10.1142/S2424905X18420047.
[11] M. Li, G. Li, B. Gonenc, et al., Towards human-controlled, real-time shape sensing based flexible needle steering for MRI-guided percutaneous therapies, Int. J. Med. Robot. Comput. Assist. Surg. 13 (2) (2017) e1762, doi:10.1002/rcs.1762.
[12] W. Park, Y. Wang, G.S. Chirikjian, Path planning for flexible needles using second order error propagation, Springer Tracts Adv. Robot. 57 (2009) 583–595.
[13] M. Khadem, C. Rossa, N. Usmani, et al., Feedback-linearization-based 3D needle steering in a Frenet-Serret frame using a reduced order bicycle model, in: American Control Conference, Seattle, USA, 2017, pp. 1438–1443.
[14] W. Park, Y. Wang, G.S. Chirikjian, The path-of-probability algorithm for steering and feedback control of flexible needles, Int. J. Robot. Res. 29 (7) (2010) 813–830, doi:10.1177/0278364909357228.
[15] P. Moreira, K.J. Boskma, S. Misra, Towards MRI-guided flexible needle steering using fiber Bragg grating-based tip tracking, in: IEEE International Conference on Robotics & Automation, Singapore, 2017, pp. 4849–4854.
[16] Z. Bo, F. Chen, Y. Miao, et al., Real-time curvature detection of a flexible needle with a bevel tip, Sensors 18 (7) (2018) 2057, doi:10.3390/s18072057.
[17] J. Xiong, Y. Gan, Z. Xia, et al., Path planning for flexible needle insertion system based on improved rapidly-exploring random tree algorithm, in: IEEE International Conference on Information and Automation (ICIA), Lijiang , China, 2015, pp. 1545–1550. 2015.

[18] S. Patil, R. Alterovitz, Interactive motion planning for steerable needles in 3D environments with obstacles, in: 3rd IEEE RASand EMBS International Conference on Biomedical Robotics and Biomechatronics, Piscataway, USA, IEEE, 2010, pp. 893–899.
[19] X. Tan, P. Yu, K.B. Lim, et al., Robust path planning for flexible needle insertion using markov decision processes, Int. J. Comput. Assist. Radiol. Surg. 13 (2) (2018) 1–13, doi:10.1007/s11548-018-1783-x.
[20] G. Li, W. Chou, Path planning for mobile robot using self-adaptive learning particle swarm optimization, Science China, Inf. Sci. 61 (5) (2018) 052204, doi:10.1007/s11432-016-9115-2.
[21] L. Yu, K. Wang, Z. Zhang, et al., Simulation-based multi-machine coordination for high-speed press line, J. Braz. Soc. Mech. Sci. Eng. 41 (7) (2019) 291, doi:10.1007/s40430-019-1775-y.
[22] H. Benyan, Z. Xingang, H. Jianda, et al., Puncture path planning for bevel-tip flexible needle based on multi-objective particle swarm optimization algorithm, Robot 37 (4) (2015) 385–394, doi:10.13973/j.cnki.robot.2015.0385.
[23] D. Hua, et al., 3D motion planning for flexible needle insertion based on rapidly-exploring random trees with environment-adaptive sampling and central angle control, J. Med. Imag. Health Inf. 9 (7) (2019) 1524–1533, doi:10.1166/jmihi.2019.2754.